Journal of
Materials Chemistry C

Accepted Manuscript

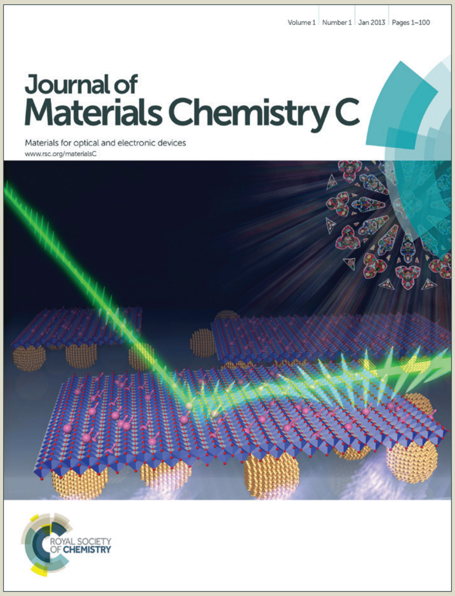

ROYAL SOCIETY OF CHEMISTRY

www.rsc.org/materialsC

Aggregation induced emission and mechanochromism in pyrenoimidazoles

Thaksen Jadhav, Bhausaheb Dhokale, Shaikh M. Mobin and Rajneesh Misra*

Department of Chemistry, Indian Institute of Technology Indore 452 017 (India)

Introduction

In recent years the research on fluorescent organic solids has gained momentum due to their wide range of applications in organic light emitting diodes (OLEDs), non-linear optics (NLO), organic lasers, and fluorescent sensors.[1] The fluorescent organic materials are extensively used in designing stimuli responsive solids called mechanochromic materials due to their applications in mechano-sensors, optical data storage, and security papers.[2] Pyrene is highly studied fluorophore for variety of applications due to its pure blue fluorescence with high quantum yield, exceptionally long fluorescence lifetime, excellent thermal stability, and high charge carrier mobility.[3] In addition, pyrene shows characteristic excimer formation in concentrated solutions and in the solid state, due to extensive π–π stacking of planar pyrene rings.[4] However pyrene excimer exhibits red shifted emission with decreased fluorescence quantum yield, which is big hurdle in solid state applications.[5] The use of sterically hindered pyrenes is promising strategy to overcome the problem of π–π stacking.[6] In this attempt Tang et al. has established a milestone by introducing the concept of aggregation induced emission (AIE). The propeller shape AIE active molecules are highly fluorescent in the solid state.[7] The tetraphenylethene (TPE) and triphenylacrylonitrile (TPAN) are AIE active molecules.[8]

Our group is involved in the design and synthesis of mechanochromic materials.[9] Recently, we have reported mechanochromic property of tetraphenylethene substituted phenanthroimidazoles.[10] We were further interested to study the effect of variation in phenanthroimidazole and TPE unit on the AIE and mechanochromic properties. Therefore we have designed and synthesized pyrene based solid state emitters **3a** and **3b** by substituting TPE and TPAN units on pyrenoimidazole, respectively. The **3a** and **3b** exhibit strong solid-state fluorescence and reversible mechano-response between blue and green.

Result and discussion

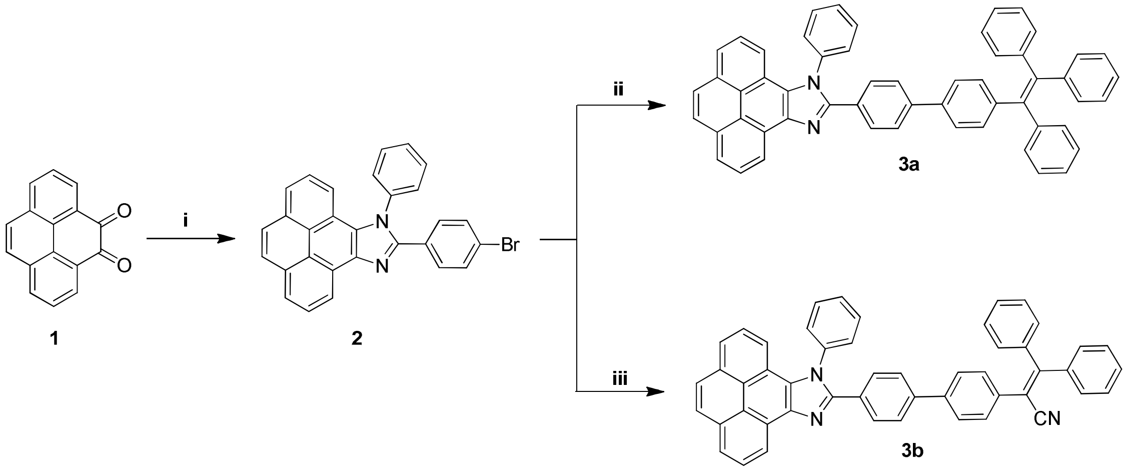

Scheme 1 Synthetic route for the pyrenoimidazoles **3a** and **3b**. (i) Aniline, 4-bromo benzaldehyde, ammonium acetate, acetic acid; (ii) 4-(1,2,2-triphenylvinyl)phenylboronic acid pinacol ester, K_2CO_3, $Pd(PPh_3)_4$, Toluene:Ethanol:Water (12.0 mL:4.0 mL:1.0 mL); (iii) 2-(4-pinacolatoboronphenyl)-3,3-diphenylacrylonitrile, K_2CO_3, $Pd(PPh_3)_4$, Toluene:Ethanol:Water (12.0 mL:4.0 mL:1.0 mL).

The condensation reaction of pyrene-4,5-dione **1** with 4-bromobenzaldehyde and aniline resulted 10-(4-bromophenyl)-9-phenyl-9H-pyreno[4,5-d]imidazole **2** in 91% yield.[11] The pyrenoimidazoles **3a** and **3b** were synthesized by the Suzuki cross-coupling reaction of bromopyrenoimidazole **2** with 4-(1,2,2-triphenylvinyl)phenylboronic acid pinacol ester and 2-(4-

pinacolatoboronphenyl)-3,3-diphenylacrylonitrile using Pd(PPh$_3$)$_4$ as catalyst in 89%, and 73% yields, respectively (Scheme 1). The 4-(1,2,2-triphenylvinyl)phenylboronic acid pinacol ester and 2-(4-pinacolatoboronphenyl)-3,3-diphenylacrylonitrile were synthesized by using reported procedures.[8,9] The pyrenoimidazoles **3a** and **3b** were purified by column chromatography followed by recrystallization. The pyrenoimidazoles **3a** and **3b** were well characterized by ^{1}H NMR, ^{13}C NMR and high resolution mass spectrometry (HRMS) techniques. The pyrenoimidazole **3a** was also characterized by single crystal X-ray analysis.

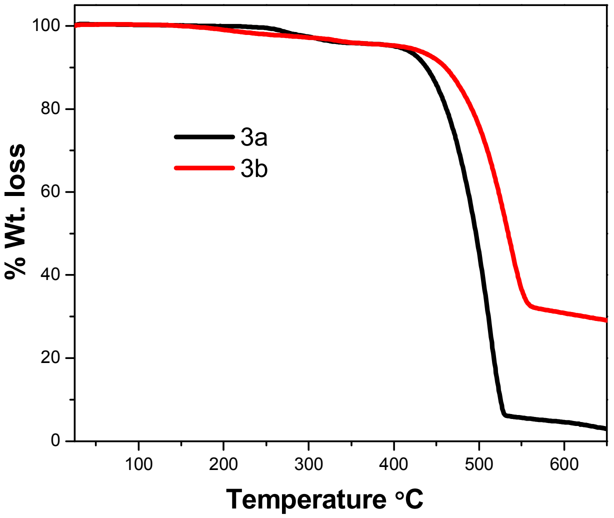

Fig. 1 Thermogravimetric analysis of **3a**, and **3b** measured at a heating rate of 10 °C/ min under nitrogen atmosphere.

The thermal stability of pyrenoimidazoles **3a** and **3b** were investigated by thermogravimetric analysis (TGA). The pyrenoimidazoles **3a** and **3b** exhibits high thermal stability. The thermal decomposition temperatures (T_d) corresponding to 5% weight loss under nitrogen atmosphere are 404 °C, and 412 °C for **3a** and **3b** respectively. This reflects the incorporation of cyano-group improves the thermal stability (Fig. 1).

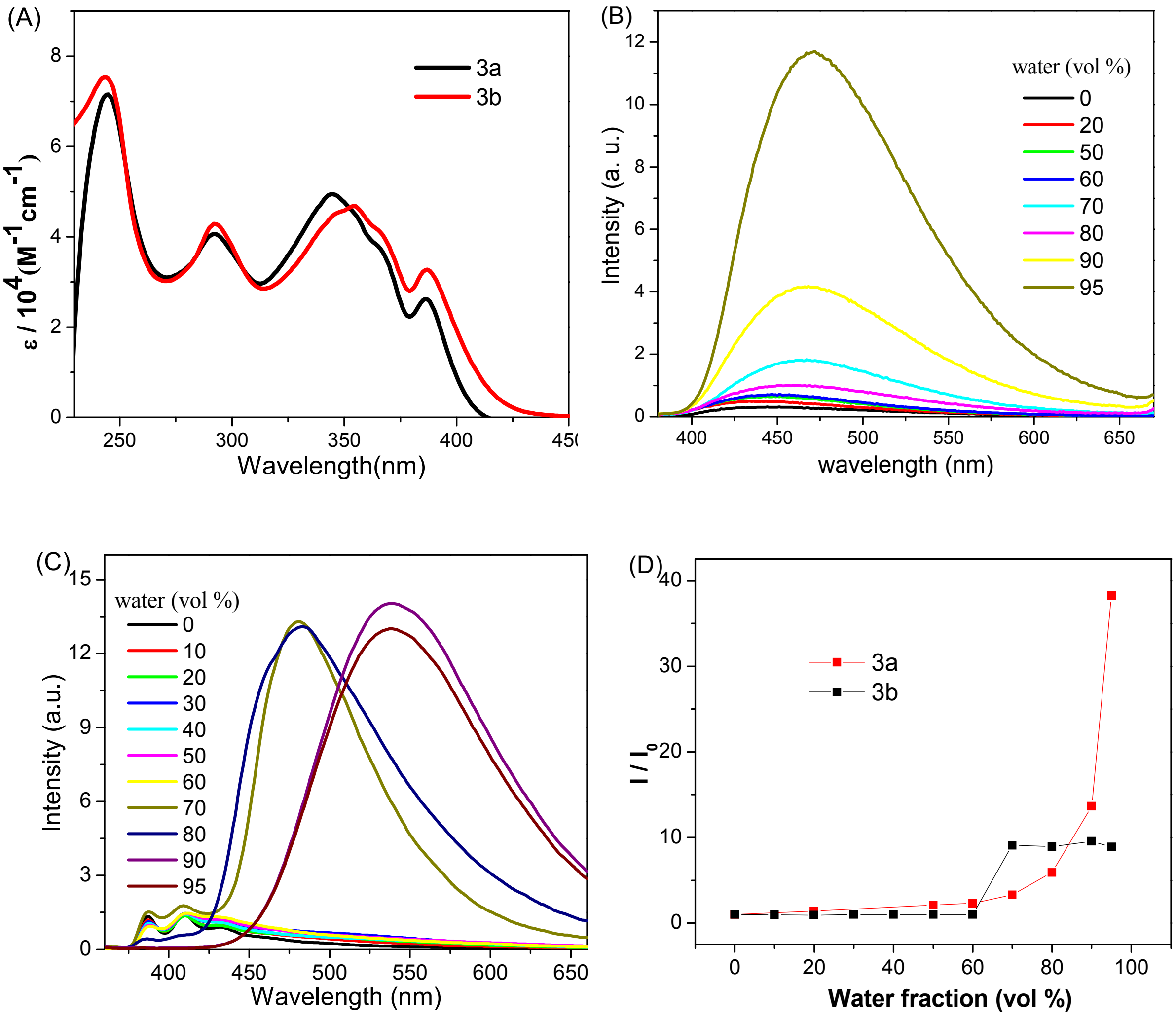

Fig. 2 (A) Electronic absorption spectra of pyrenoimidazoles **3a** and **3b** recorded in THF. (B) Fluorescence spectra of **3a**, and (C) **3b** in THF-water mixtures with different water fractions. (D) Plot of fluorescence intensity (PL) vs. % of water fraction (f_w). Luminogen concentration: 10 μM; excitation wavelength: 340 nm; intensity calculated at λ_{max}.

The electronic absorption spectra of the pyrenoimidazoles **3a** and **3b** are shown in Fig. 2, and the data are summarized in Table S2. The pyrenoimidazoles **3a** and **3b** exhibit similar absorption behavior with small red shift in the absorption spectra of **3b**. The absorption spectra of **3a** and **3b** show broad absorption band between 230–400 nm with absorption maxima around

243 nm, 292 nm, 350 nm and 387 nm. The absorption band between 310-410 nm corresponds to π-π^* transitions localized on the pyrenoimidazoles.[12] This long wavelength absorption band is significantly red shifted than corresponding TPE substituted phenanthroimidazole derivative.[10] The pyrenoimidazoles **3a** and **3b** are weakly fluorescent in solutions, this can be ascribed to nonradiative decay of the excited state due to free molecular rotations of tetraphenylethylene unit in the solution. The fluorescence spectra of pyrenoimidazole **3b** shows vibronic pattern whereas the vibronic pattern disappears in pyrenoimidazole **3a**. The effect of solvent polarities on the absorption and fluorescence spectra was studied in solvents toluene, chloroform, dichloromethane, and tetrahydrofuran. The pyrenoimidazoles **3a** and **3b** are insoluble in highly polar (acetonitrile) and non-polar (cyclohexane) solvents. The solvatochromic study shows negligible changes on both absorption and fluorescence spectra (Fig. S2 and S3 and Table S3). This reveals that there is less charge polarization in ground as well as excited state.

To check the AIE behavior of pyrenoimidazoles **3a** and **3b**, the absorption and fluorescence spectra in THF–water mixtures with different water fraction were studied. The small aggregates were prepared in THF by gradual increase in the water fraction. The pyrenoimidazoles **3a** and **3b** are weakly fluorescent in pure tetrahydrofuran and becomes highly fluorescent at higher water fraction which reveals these pyrenoimidazoles are AIE active (Fig. 2). The different percentage of water fraction was required for pyrenoimidazoles **3a** and **3b** to start AIE effect. The pyrenoimidazole **3a** requires more than 80% water fraction, whereas pyrenoimidazole **3b** requires more than 60% water fraction. The poor fluorescence of pyrenoimidazoles **3a** and **3b** in THF was enhanced in aggregated suspension (95% water fraction) by 38 and 9 folds, respectively (Fig. 2). The quantitative estimation of the AIE process was obtained by calculating the fluorescence quantum yields, in the mixture of water and THF in various proportions, using 9,10-diphenylanthracene as standard. In pure THF solution, pyrenoimidazoles **3a** and **3b** exhibit poor fluorescence with quantum yield 0.0017 and 0.0043 respectively, which was increased to 0.0460 and 0.0927 in the aggregated state (95 % aqueous).

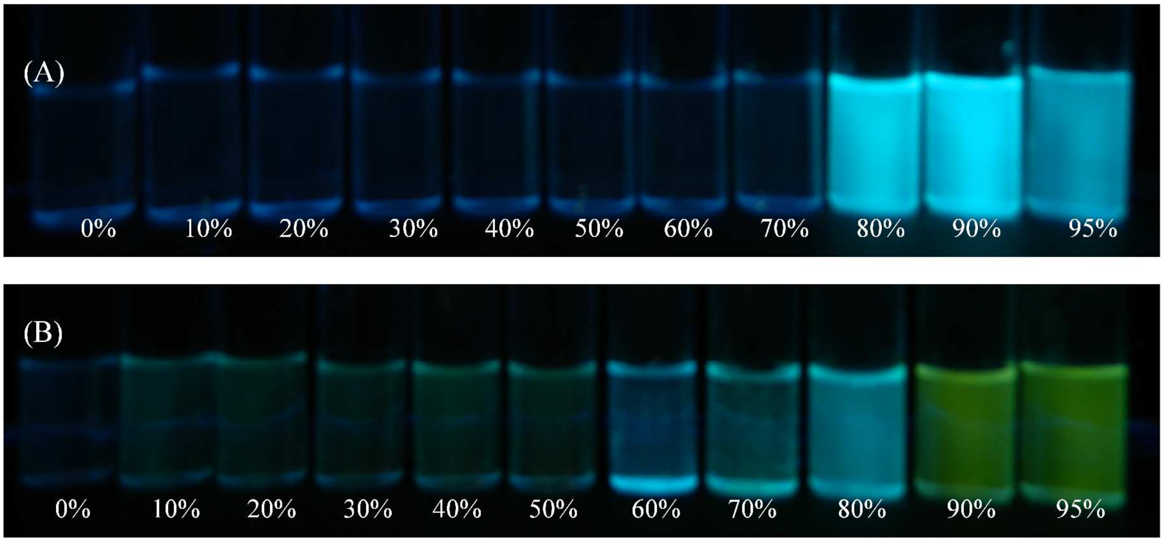

Fig. 3 Photographs of **3a** (A) and **3b** (B) in THF–water mixtures with different water fractions (10 μM) under 365 nm UV illumination.

The images of pyrenoimidazoles **3a** and **3b** in THF–water mixture with different water fractions under UV illumination are shown in Fig. 3. The pyrenoimidazole **3b** emits different color light at different water fraction, the aggregates formed at 70-80% water fraction emits blue color light (λ = 482 nm), whereas aggregates formed at more than 90% water fraction emits yellow light (λ = 539 nm). The size of different nano-aggregates of pyrenoimidazoles **3a** and **3b** at different water fraction was studied by dynamic light scattering (DLS). The DLS study of **3b** shows average diameter of 325 nm at 70% water fraction and 145 nm at 95% water fraction (Fig. 4). The nano-aggregates of **3a** exhibit average diameter of 420 nm at 90% water fraction which is larger compared to **3b** (Fig. S5). The larger average diameter of **3a** nano-aggregates compared to **3b** may leads to the lower quantum yield in **3a**. This may be due to the more contribution of molecules on the surface of the nano-aggregates in the emission intensity.[12] The AIE behavior was further explored by studying the absorption spectra in the THF–water mixtures (10 μM) (Fig. S4). The absorption spectra of pyrenoimidazole **3a** at 80% water fraction, whereas pyrenoimidazole **3b** at 60% water fraction started to show light scattering by the nanoaggregate suspension in the THF–water mixtures.

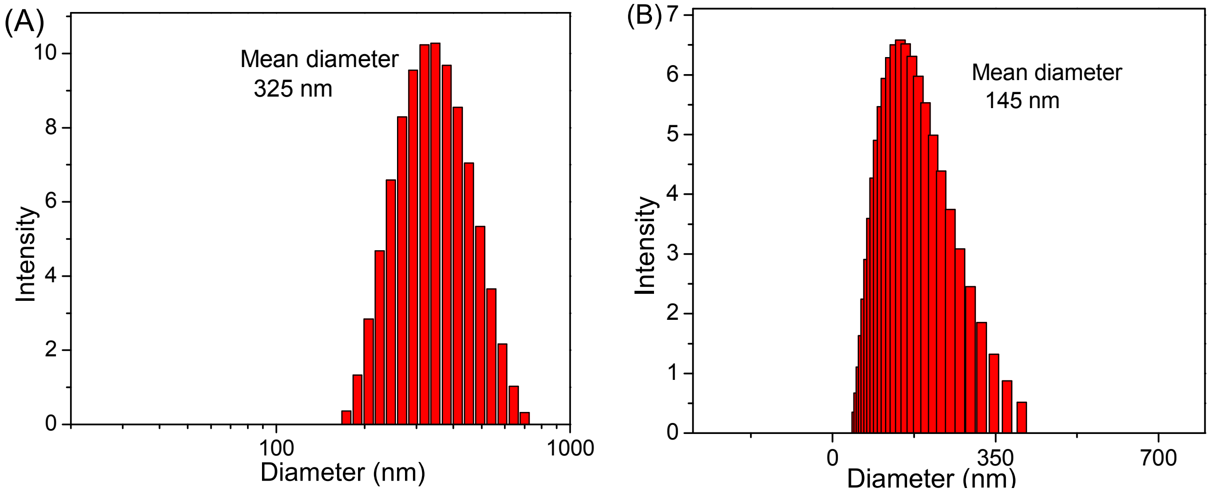

Fig. 4 The particle size distributions of **3b** in THF–water mixture (A) at 70% (f_w) and (B) at 95% (f_w).

The mechanochromic properties of pyrenoimidazoles **3a** and **3b** were studied by solid state emission spectroscopy. In the pristine form **3a** shows blue light emission at 461 nm, and **3b** show sky blue emission at 473 nm. Upon grinding using a spatula or pestle **3a** and **3b** solids exhibit drastic change in the emission behavior and exhibit yellowish green emission with emission maxima at 499 nm and 510 nm respectively (Fig. 5). This mechanochromic effect is highly reversible in nature and can be reverted to its original color by annealing or fuming with solvent vapors. The ground sample of **3a** upon annealing at 200 °C for 15 min or fuming with dichloromethane vapor for 2 min, restored to the original blue emission. Whereas in ground sample of **3b**, annealing at 220 °C was required for 15 min to restore the original blue emission whereas fuming with solvent vapor does not restore to its original color completely.

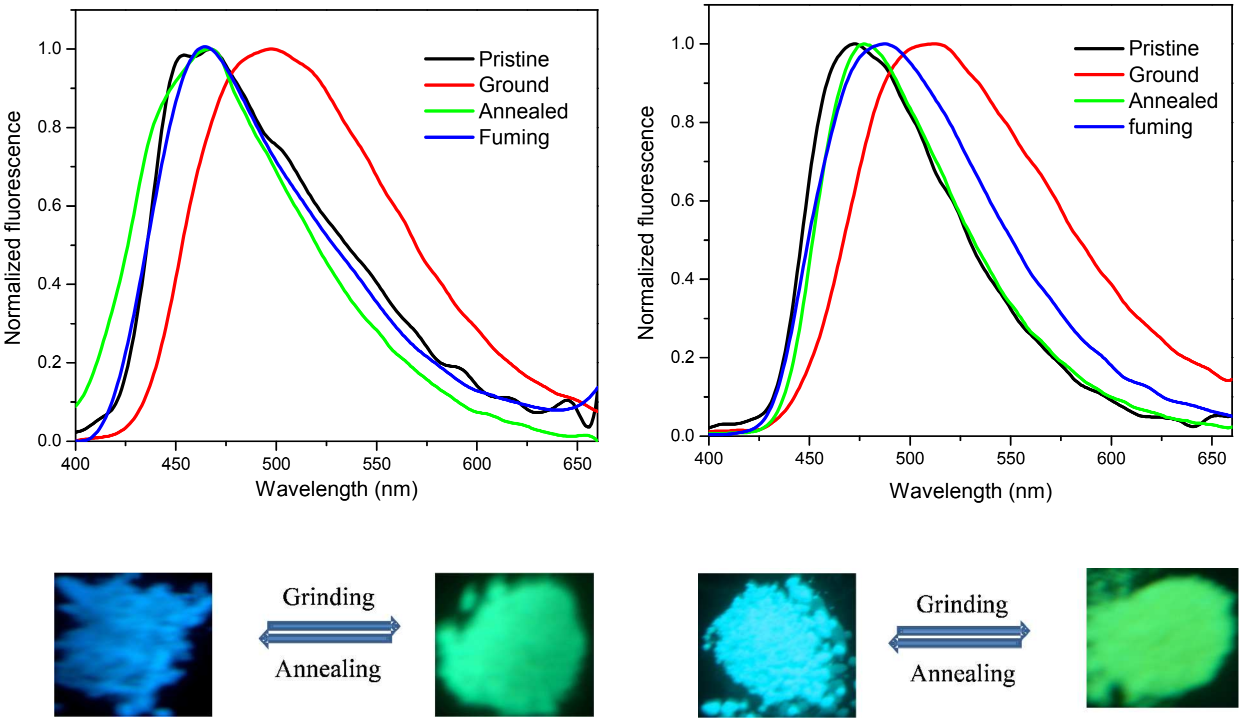

Fig. 5 Emission spectra of **3a** (left) and **3b** (right) as Pristine, Ground and Heated solids and photograph taken under 365 nm UV illumination.

In order to understand the emission behavior under different stimuli, we have recorded absorption spectra in the solid state (Fig. S6). The pristine form of pyrenoimidazole **3a** and **3b** absorbs at 417 nm and 427 nm respectively which upon grinding exhibits bathochromic shift and absorbs at 446 nm and 437 nm, respectively. The bathochromic shift in absorption and emission suggests the enhanced conjugation, which can be attributed to the transformation of twisted conformation in pristine form to comparatively planar conformation in the ground form.

The pristine, ground and fumed forms of pyrenoimidazoles **3a** and **3b** were studied using powder X-ray diffraction (PXRD) (Fig. 6). The diffraction patterns for pristine samples show sharp peaks, which is characteristic property of the crystalline state. The pristine samples upon grinding show broad diffuse band for **3a** and peak broadening in **3b** which indicates increased amorphous nature. The ground samples after fuming with dichloromethane restore the sharp peaks, suggesting regeneration of the crystalline nature. The PXRD study reveals that the morphological change from the crystalline state to the amorphous state and vice versa is associated with the mechanochromism in pyrenoimidazoles **3a** and **3b**.

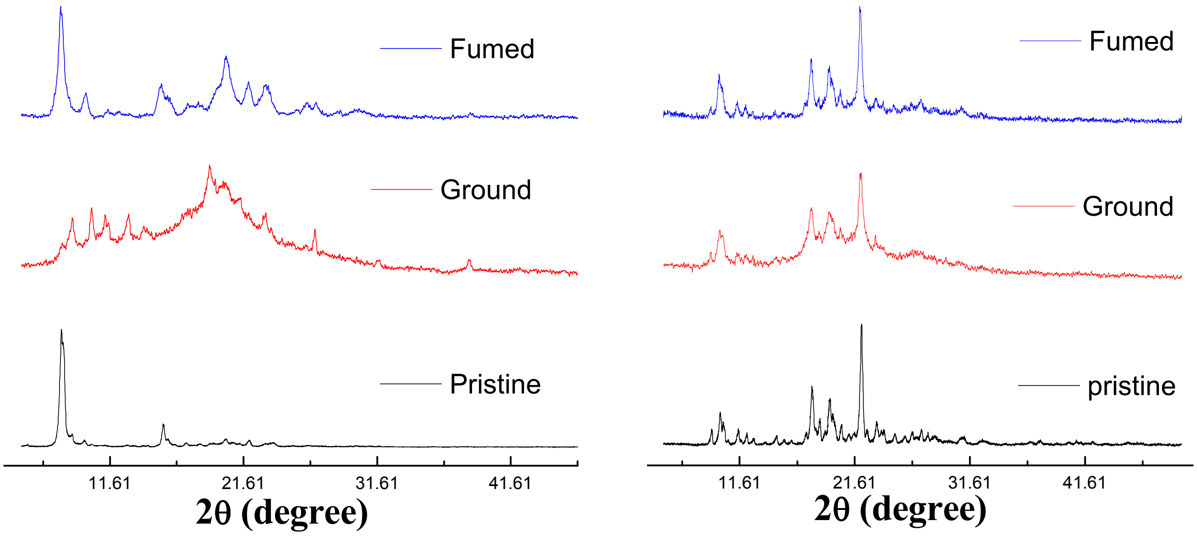

Fig. 6 PXRD curves of **3a** (left) and **3b** (right) in Synthesized, Ground and Fumed form.

The single crystal X-ray structure of **3a** provides insight into the AIE. Generally, the pyrene unit containing fluorophores were known for planar and extensive π---π staking interactions, but the crystal structure of **3a** exhibits twisted conformation of phenyl rings of TPE unit (Fig. 7). This twisted conformation suppresses the π---π staking effect of pyrene and supports AIE active nature, also twisting in phenyl rings supports the intramolecular rotations in solution leading to poor fluorescence. The packing diagram of **3a e**xhibits intermolecular C-H---π interactions. Two mutual C-H---π interactions between two molecule via C(45)-H(45)---π(pyrene) And C(19)-H(19)---π (phenyl) to form a dimeric framework in head to tail fashion. Such dimers are connected to each other via C-H---π interaction C(42)-H(42)---π(pyrene) forming 2D staircase shaped framework (Fig. 7). Thus, packing diagram reveals the absence of strong π---π staking in pyrene unit.

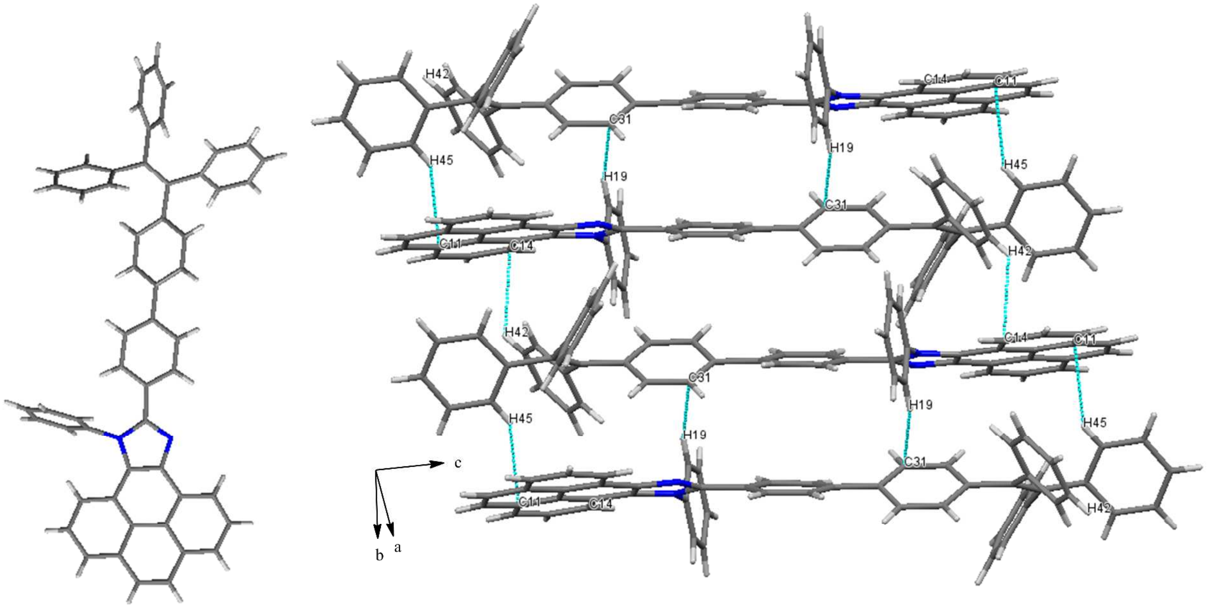

Fig. 7 Crystal structure and C-H---π interactions assisted crystal packing of **3a**.

The geometry optimized and electronic structures of the pyrenoimidazoles **3a** and **3b** were obtained by density functional theory (DFT) calculations. The DFT calculations were performed at the B3LYP/6-31G(d) level.[13] The geometry optimized structures show highly twisted conformation. The contours of the highest occupied molecular orbital (HOMO) and lowest unoccupied molecular orbital (LUMO) of pyrenoimidazoles **3a** and **3b** are shown in Fig. 8. The HOMO orbitals are localized over pyrenoimidazole part in **3a** and **3b**. In case of **3a** the

LUMO orbital is localized on the TPE, imidazole and some part on pyrene unit, whereas in **3b** the LUMO orbital is localized only on the triphenylacrylonitrile. The replacement of phenyl in TPE with cyano-group in **3b** leads to stabilization of both the HOMO and LUMO. The extent of stabilization of LUMO is more pronounced compared to HOMO, which leads to low HOMO-LUMO gap in **3b** compared to **3a**. This indicates the stronger donor-acceptor interaction in **3b** compared to **3a**.

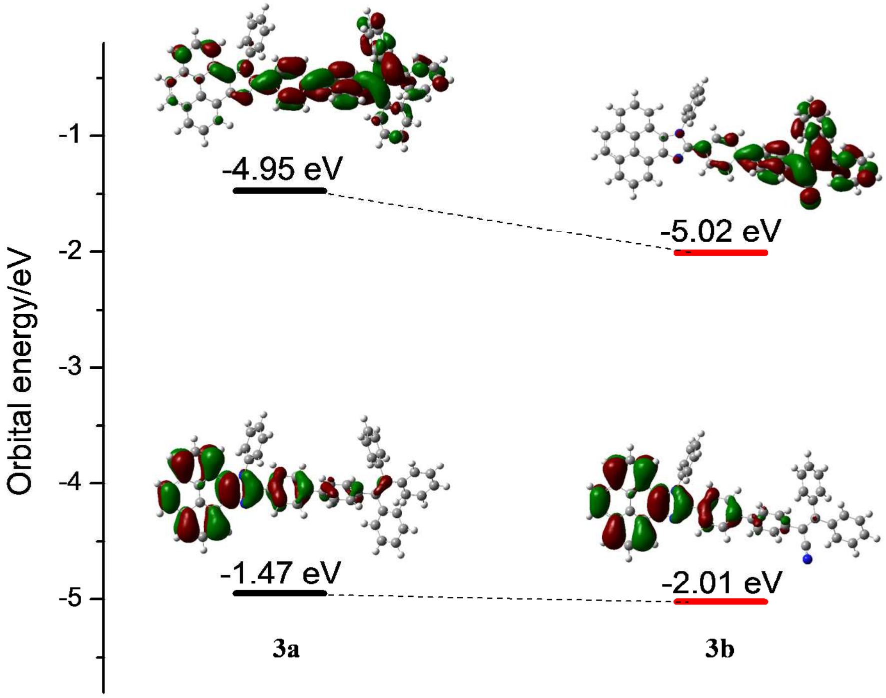

Fig. 8 Correlation diagram showing the HOMO, and LUMO wave functions and energies of the pyrenoimidazoles **3a** (left) and **3b** (right).

Conclusion

In summary, we have designed and synthesized pyrenoimidazoles **3a** and **3b** by the Pd-catalyzed Suzuki cross-coupling reaction of bromopyrenoimidazole **2** with 4-(1,2,2-triphenylvinyl)phenylboronic acid pinacol ester and 2-(4-pinacolatoboronphenyl)-3,3-

diphenylacrylonitrile. The single crystal structure and packing diagram of **3a** reveals twisted conformation and absence of strong π---π staking in pyrene units which results in fluorescent solids. The strong aggregation induced emission (AIE) and different AIE behavior was observed for **3a** and **3b**. The **3b** shows different colored emission at different water fraction which can be ascribed to the different sized nanoaggregates formation. The pyrenoimidazoles **3a** and **3b** exhibit reversible mechanochromic behavior with color contrast between blue and green. The solid state absorption, emission and powder XRD study reveals that, the transformation of twisted crystalline state to planar amorphous state is the main cause for mechanochromism in pyrenoimidazoles **3a** and **3b**. The optoelectronic applications of these materials are currently ongoing in our laboratory.

Experimental details:

General methods

Chemicals were used as received unless otherwise indicated. All oxygen or moisture sensitive reactions were performed under nitrogen/argon atmosphere. ^{1}H NMR (400 MHz), and ^{13}C NMR (100MHz) spectra were recorded on on the Bruker Avance (III) 400 MHz instrument by using $CDCl_3$. ^{1}H NMR chemical shifts are reported in parts per million (ppm) relative to the solvent residual peak ($CDCl_3$, 7.26 ppm). Multiplicities are given as: s (singlet), d (doublet), t (triplet), q (quartet), dd (doublet of doublets), dt (doublet of triplets), m (multiplet), and the coupling constants, *J*, are given in Hz. ^{13}C NMR chemical shifts are reported relative to the solvent residual peak ($CDCl_3$, 77.36 ppm. Thermogravimetric analyses were performed on the Metler Toledo Thermal Analysis system. UV-visible absorption spectra were recorded on a Carry-100 Bio UV-visible Spectrophotometer. Emission spectra were taken in a fluoromax-4p fluorimeter from HoribaYovin (model: FM-100). The excitation and emission slits were 2/2 nm for the emission measurements. All of the measurements were done at 25 °C. HRMS were recorded on Brucker-Daltonics, micrOTOF-Q II mass spectrometer.

Synthesis:

Synthesis and characterization of intermediate 2:

2: The pyrene-4,5-dione (9.6 mmol), 4-bromobenzaldehyde (9.6 mmol), aniline (14.4 mmol), and ammonium acetate (96.1 mmol) in glacial acetic acid (50 mL) refluxed for 12 h under an argon atmosphere. After cooling to room temperature, a pale yellow mixture was obtained and poured into a methanol solution under stirring. The separated solid was filtered off, washed with 30 ml water, and dried to give compound **2** as off white solid. Yield: 91.0 %. ^{1}H NMR (400 MHz, $CDCl_3$, 25 °C): δ 9.09 (dd, 1H, *J*=1.2, 8 Hz), 8.21 (dd, 1H, *J*=1.2, 8 Hz), 8.10-8.16 (m, 2H), 8.03-8.06 (m, 2H), 7.63-7.71 (m, 4H), 7.58-7.61 (m, 2H), 7.53 (dt, 2H, *J*=2, 8 Hz), 7.45 (dt, 2H, *J*=2, 8 Hz), 7.39 (dd, 1H, *J*=0.8, 8 Hz) ppm; HRMS (ESI): calcd. for $C_{19}H_{17}BrN_2$: 473.0648 $(M+H)^+$, found 473.0647.

Synthesis and Characterization of 3a and 3b:

3a: $Pd(PPh_3)_4$ (0.004 mmol) was added to a well degassed solution of 10-(4-bromophenyl)-9-phenyl-9H-pyreno[4,5-d]imidazole (**2**) (0.4 mmol), 4-(1,2,2-triphenylvinyl)phenylboronic acid pinacol ester (0.48 mmol), K_2CO_3(1.2 mmol) in a mixture of toluene (12 mL)/ ethanol (4.0 mL)/ H_2O (1.0 mL). The resulting mixture was stirred at 80 ºC for 24 h under argon atmosphere. After cooling, the mixture was evaporated to dryness and the residue subjected to column chromatography on silica (Hexane-DCM 25:75 in vol.) to yield the desired product **3a** as colorless powder. The compound was recrystalized from DCM:ethanol (8:2) mixtures. Yield:

89.0%. ^{1}H NMR (400 MHz, $CDCl_3$, 25 °C): δ 9.13 (dd, 1H, *J*=1.2, 8 Hz), 8.20 (dd, 1H, *J*=1.2, 8 Hz), 8.10-8.16 (m, 2H), 8.03-8.05 (m, 2H), 7.61-7.70 (m, 8H), 7.52 (dt, 2H, *J*=4, 8 Hz), 7.34-7.41 (m, 4H), 7.02-7.14 (m, 17H) ppm; ^{13}C NMR (100 MHz, $CDCl_3$, 25 °C): δ 150.8, 143.7, 143.7, 143.6, 143.2, 141.3, 140.8, 140.4, 138.9, 138.0, 137.8, 135.2, 132.2, 131.8, 131.7, 131.4, 131.3, 130.2, 129.9, 129.6, 129.2, 128.9, 127.9, 127.9, 127.8, 127.7, 127.6, 127.5, 126.5, 126.5, 126.4, 126.3, 126.1, 125.3, 124.5, 124.3, 123.5, 122.8, 122.4, 119.8, 117.9, 0.00 ppm; HRMS (ESI): calcd. for $C_{55}H_{36}N_2$: 725.2951 $(M+H)^+$, found 725.2954.

3b: $Pd(PPh_3)_4$ (0.004 mmol) was added to a well degassed solution of 10-(4-bromophenyl)-9-phenyl-9H-pyreno[4,5-d]imidazole (**2**) (0.4 mmol), 2-(4-pinacolatoboronphenyl)-3,3-diphenylacrylonitrile (0.48 mmol), K_2CO_3(1.2 mmol) in a mixture of toluene (12 mL)/ ethanol (4.0 mL)/ H_2O (1.0 mL). The resulting mixture was stirred at 80 ºC for 24 h under argon atmosphere. After cooling, the mixture was evaporated to dryness and the residue subjected to column chromatography on silica (Hexane-DCM 15:85 in vol.) to yield the desired product **3b** as greenish yellow powder. The compound was recrystalized from DCM:ethanol (8:2) mixtures. Yield: 73.0 %. ^{1}H NMR (400 MHz, $CDCl_3$, 25 °C): δ 9.13 (dd, 1H, *J*=1.2, 8 Hz), 8.10-8.22 (m, 3H), 8.03-8.06 (m, 2H), 7.62-7.73 (m, 8H), 7.53 (d, 2H, *J*= 8 Hz), 7.70-7.49 (m, 8H), 7.31-7.34 (m, 2H), 7.21-7.29 (m, 3H), 7.05-7.07 (m, 2H) ppm; ^{13}C NMR (100 MHz, $CDCl_3$, 25 °C): δ 157.8, 140.4, 140.2, 140.0, 139.1, 138.8, 134.1, 132.2, 131.7, 130.8, 130.3, 130.2, 130.0, 129.8, 129.2, 129.1, 128.9, 128.5, 128.4, 128.0, 127.6, 126.9, 126.7, 126.4, 125.3, 124.6, 124.4, 123.6, 122.9, 122.4, 120.0, 119.8, 118.0, 111.1, 0.00 ppm; HRMS (ESI): calcd. for $C_{50}H_{31}N_3+H^+$: 674.2591 $(M+H)^+$, found 674.2599.

Fluorescence quantum yields (ϕ_F)

The fluorescence quantum yields for AIE study (ϕ_F) were calculated using 9,10-diphenylanthracene as standard in various THF-water mixtures by the steady-state comparative method.

$$\phi_F = \phi_{st} \times S_u/S_{st} \times A_{st} / A_u \times n^2_{Du}/n^2_{Dst}$$

Where ϕ_F is the emission quantum yield of the sample, ϕ_{st} is the emission quantum yield of the standard, A_{st} and A_u represent the absorbance of the standard and sample at excitation wavelength, respectively. The S_{st} and S_u are the integrated emission band areas of the standard and sample, respectively, and n_{Dst} and n_{Du} are the solvent refractive index of the standard and sample. The u and st refer to the unknown and standard, respectively.

Supplementary data

Electronic supplementary information (ESI) available: UV-vis spectra, mechanochromic effect, NMR spectra, computational data and crystal structural data for **3a**. Crystallographic data for the structure **3a** in this paper have been deposited with the Cambridge Crystallo- graphic Data Centre as supplementary publication nos. CCDC **1409647**.

Acknowledgments

We acknowledge the support by DST, and CSIR Govt. of India, New Delhi. T J thanks UGC, B D thanks to CSIR New Delhi for their fellowships. We acknowledge Sophisticated Instrumentation Centre (SIC) facility, IIT Indore.

References:

1 (a) S. R. Forrest, *Org. Electron.*, 2003, **4**, 45; (b) M. Shimizu and T. Hiyama, *Chem.–Asian J.*, 2010, **5**, 1516; (c) T. P. I. Saragi, T. Spehr, A. Siebert, T. Fuhrmann-Lieker and J. Salbeck, *Chem Rev.*, 2007, **107**, 1011; (d) M. D. McGehee and A. J. Heeger, *Adv. Mater.*, 2000, **12**, 1655; (e) I. D. W. Samuel and G. A. Turnbull, *Chem. Rev.*, 2007, **107**, 1272; (f) H. Xu, R. Chen, Q. Sun, W. Lai, Q. Su, W. Huang and X. Liu, *Chem. Soc. Rev.*, 2014, **43**, 3259–3302; (g) J. Zaumseil and H. Sirringhaus, *Chem. Rev.*, 2007, **107**, 1296; (h) F. Cicoira and C. Santato, *Adv. Funct. Mater.*, 2007, **17**, 3421; (i) X. Y. Liu, D. R. Bai and S. Wang, *Angew. Chem.*, 2006, **118**, 5601.

2 (a) Z. Chi, X. Zhang, B. Xu, X. Zhou, C. Ma, Y. Zhang, S. Liua and J. Xu, *Chem. Soc. Rev.*, 2012, **41**, 3878–3896; (b) Y. Sagara and T. Kato, *Nat. Chem.*, 2009, **1**, 605; (c) X. L. Luo, J. N. Li, C. H. Li, L. P. Heng, Y. Q. Dong, Z. P. Liu, Z. S. Bo and B. Z. Tang, *Adv. Mater.*, 2011, **23**, 3261; (d) Y. J. Dong, B. Xu, J. B. Zhang, X. Tan, L. J. Wang, J. L. Chen, H. G. Lv, S. P. Wen, B. Li, L. Ye, B. Zou and W. J. Tian, *Angew. Chem. Int. Ed.*, 2012, **51**, 10782; (e) D. A. Davis, A. Hamilton, J. L. Yang, L. D. Cremar, D. Van Gough, S. L. Potisek, M. T. Ong, P. V. Braun, T. J. Martinez, S. R. White, J. S. Moore and N. R. Sottos, *Nature*, 2009, **459**, 68.

3 (a) Y. O. Lee, T. Pradhan, S. Yoo, T. H. Kim, J. Kim and J. S. Kim, *J. Org. Chem.,* 2012, **77**,11007; (b) T. M. Figueira-Duarte, K. Mullen, *Chem. Rev.*, 2011, **111**, 7260–7314; (c) J. R. Lakowicz, Principles of Fluorescence Spectroscopy, Plenum press, New York, 1999; (d) J. B. Birks, *Photophysics of Aromatic Molecules*, Wiley-Interscience, London, 1970; (e) B. Dhokale, T. Jadhav, S. M. Mobin and R. Misra, *RSC Adv.*, 2015, **DOI:** 10.1039/C5RA11433K.

---

4 (a) T. Forster and K. Kasper, *Z. Phys. Chem.* 1954, **1**, 275; (b) J. B. Birks, D. J. Dyson and I. H. Munro, *Proc. R. Soc. London Ser. A* 1963, **275**, 575; (c) K. A. Zachariasse, *Trends Photochem. Photobiol*. 1994, **3**, 211.

5 (a) J. N. Moorthy, P. Natarajan, P. Venkatakrishnan, D. F. Huang and T. J. Chow, *Org. Lett.*, 2007, **9**, 5215–5218; (b) P. Sonar, M. S. Soh, Y. H. Cheng, J. T. Henssler and A. Sellinger, *Org. Lett.*, 2010, **12**, 3292–3295; (c) W. Sotoyama, H. Sato, M. Kinoshita, T. Takahashi, A. Matsuura, J. Kodama, N. Sawatari and H. Inoue, *SID Digest*, 2003, **45**, 1294–1295.

6 (a) T. M. Figueira-Duarte, S. C. Simon, M. Wagner, S. I. Drtezhinin, K. A. Zachariasse and K. Mullen, *Angew. Chem., Int. Ed.*, 2008, **47**, 10175–10178; (b) T. M. Figueira-Duarte, P. G. Del Rosso, R. Trattnig, S. Sax, E. J. W. List and K. Mullen, *Adv. Mater.*, 2010, **22**, 990–993; (c) J. Y. Hu, M. Era, M. R. J. Elsegood and T. Yamato, *Eur. J. Org. Chem.*, 2010, 72–79; (d) L. Zophel, D. Beckmann, V. Enkelmann, D. Chercka, R. Rieger and K. Mullen, *Chem. Commun.*, 2011, **47**, 6960–6962.

7 (a) J. D. Luo, Z. L. Xie, J. W. Y. Lam, L. Cheng, H. Y. Chen, C. F. Qiu, H. S. Kwok, X. W. Zhan, Y. Q. Liu, D. B. Zhu and B. Z. Tang, *Chem. Commun.*, 2001, 1740; (b) Y. Li, T. Liu, H. Liu, M. Z. Tian, and Y. Li, Acc. Chem. Res., 2014, 47, 1186.

8 (a) Y. Dong, J. W.Y. Lam, A. Qin, J. Liu,Z. Li, B. Z.Tang, J. Sun and H. S. Kwok, *Appl. Phys. Lett.*, 2007, **91**, 011111; (b) J. Huang, X. Yang, J. Wang, C. Zhong, L. Wang, J. Qin and Z. Li, *J. Mater. Chem.*, 2012, **22**, 2478; (c) N. Zhao, Z. Y. Yang, J. W. Y. Lam, H. H. Y. Sung, N. Xie, S. J. Chen, H. M. Su, M. Gao, I. D. Williams, K. S. Wong and B. Z. Tang, *Chem. Commun.*, 2012, **48**, 8637; (d) J. Wang, J. Mei, R. Hu, J. Z. Sun, A. Qin and B. Z. Tang, *J. Am. Chem. Soc.*, 2012, **134**, 9956; (e) S. Wang, W. J. Oldham, R. A. Hudack and G. C. Bazan, *J. Am. Chem. Soc.* 2000, **122**, 5695; (f) W. Z. Yuan, Y. Gong, S. Chen, X. Y. Shen, J. W. Y. Lam, P. Lu, Y. Lu, Z. Wang,

R. Hu, N. Xie, H. S. Kwok, Y. Zhang, J. Z. Sun and B. Z. Tang, *Chem. Mat.* 2012, **24**, 1518; (g) W. Z. Yuan, Y. Tan, Y. Y. Gong, P. Lu, J. W. Y. Lam, X. Y. Shen, C. Feng, H. H. Y. Sung, Y. Lu, I. D. Williams, J. Z. Sun, M. Y. Zhang and B. Z. Tang, *Adv. Mater.*, 2013, **25**, 2837–2843; (h) Y. Gong, Y. Tan, J. Liu, P. Lu, C. Feng, W. Yuan, Y. Lu, J. sun, G. He and Y. Zhang, *Chem. Commun.*, 2013, **49**, 4009.

9 (a) T. Jadhav, B. Dhokale, S. M. Mobin and R. Misra, *RSC Adv.*, 2015, **5**, 29878-29884; (b) P. Gautam, R. Maragani, S. M. Mobin and R. Misra, *RSC Adv.*, 2014,**4**, 52526; (c) T. Jadhav, B. Dhokale and R. Misra, *J. Mater. Chem. C*, DOI: 10.1039/c5tc01871d.

10 R. Misra, T. Jadhav, B. Dhokale and S. M. Mobin, *Chem. Commun.*, 2014, **50**, 9076-9078.

11 X. Yi, P. Yang, D. Huang and J. Zhao, *Dyes and Pigments*, 2013, **96**, 104-115.

12 X. Zhang, Z. Chi, B. Xu, C. Chen, X. Zhou, Y. Zhang, S. Liu and J. Xu, *J. Mater. Chem.*, 2012, **22**, 18505–18513.

13 (a) M. J. Frisch, G. W. Trucks, H. B. Schlegel, G. E. Scuseria, M. A. Robb, J. R. Cheeseman, G. Scalmani, V. Barone, B. Mennucci, G. A. Petersson, H. Nakatsuji, M. Caricato, X. Li, H. P. Hratchian, A. F. Izmaylov, J. Bloino, G. Zheng, J. L. Sonnenberg, M. Hada, M. Ehara, K. Toyota, R. Fukuda, J. Hasegawa, M. Ishida, T. Nakajima, Y. Honda, O. Kitao, H. Nakai, T. Vreven, J. A. Jr. Montgomery, J. E. Peralta, F. Ogliaro, M. Bearpark, J. J. Heyd, E. Brothers, K. N. Kudin, V. N. Staroverov, R. Kobayashi, J. Normand, K. Raghavachari, A. Rendell, J. C. Burant, S. S. Iyengar, J. Tomasi, M. Cossi, N. Rega, N. J. Millam, M. Klene, J. E. Knox, J. B. Cross, V. Bakken, C. Adamo, J. Jaramillo, R. Gomperts, R. E. Stratmann, O. Yazyev, A. J. Austin, R. Cammi, C. Pomelli, J. W. Ochterski, R. L. Martin, K. Morokuma, V. G. Zakrzewski, G. A. Voth, P. Salvador, J. J. Dannenberg, S. Dapprich, A. D. Daniels, O. Farkas, J. B. Foresman, J. V. Ortiz, J. Cioslowski, D. J. Fox, Gaussian 09, revision A.02; Gaussian,

---

Inc.: Wallingford, CT, 2009; b) C. Lee, W. Yang and R. G. Parr, *Phys. Rev. B*, 1988, **37**, 785; c) A. D. *J.* Becke, *Chem. Phys.*, 1993, **98**, 1372.

Toc

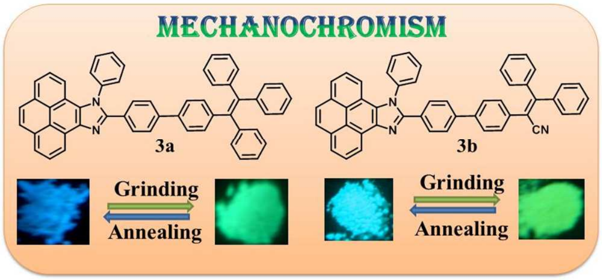

Abstract

Pyrene based solid state emitters **3a** and **3b** were designed and synthesized by the Pd-catalyzed Suzuki cross-coupling reaction of bromopyrenoimidazole **2** with 4-(1,2,2-triphenylvinyl)phenylboronic acid pinacol ester and 2-(4-pinacolatoboronphenyl)-3,3-diphenylacrylonitrile. The single crystal X-ray structure of **3a** was reported and reveals the twisted conformation. Their photophysical, aggregation induced emission (AIE) and mechanochromic properties were studied. The pyrenoimidazoles **3a** and **3b** exhibit strong AIE. The **3b** shows different colored emission with varying water fraction. The **3a** and **3b** exhibit reversible mechanochromic behavior with colors contrast between blue and green. The enhanced conjugation and increasing amorphous nature after grinding are associated with mechanochromism in pyrenoimidazoles **3a** and **3b**.